ELSEVIER

Thermochimica Acta 317 (1998) 183–192

thermochimica
acta

Characterization, kinetics and mechanism of thermal decomposition of photosubstituted ethylenediamine complexes of molybdate(IV) and tungstate(IV) with chromium(III).

S.I. Ali*, Kowsar Majid

Department of Chemistry, Jamia Millia Islamia, New Delhi-110 025, India

Received 5 January 1998; received in revised form 20 May 1998; accepted 22 May 1998

Abstract

Photoinitiated substitution complexes of $[M(CN)_8]^{4-}$ (where M= Mo(IV) or W(IV)) and ethylenediamine with chromium(III) have been synthesized and characterized. On the basis of elemental analysis, the complexes have been assigned formulas as folows:

$Cr[Mo(CN)(C_2H_8N_2)(OH)_6]\cdot 2H_2O$ **I** for Mo(IV); and

$Cr[W(C_2H_8N_2)(O_2)(OH)_3]\cdot H_2O$ **II** for W(IV)

The characteristic IR absorption peaks for different entities present support the assigned formulas. Complex **I** shows the absorption peaks due to $\nu(C\equiv N)$ stretching bond, NH asymmetric deformation, NH symmetric deformation and NH_3 rocking mode showing the presence of cyanide and ethylenediamine. The loss of the absorption peak due to $\nu(C\equiv N)$ stretching in the spectra of complex **II** confirms the substitution of all the cyanide ligands. The thermal degradation of the complexes has been studied by TG and DSC techniques. Both the complexes have a similar thermal decomposition behavior: involving expulsion of water molecules in the first step followed by the expulsion of other ligands. Kinetics and a thermal decomposition mechanism have been proposed for each complex. Thermodynamic parameters such as activation energy (E_a), pre-exponential factor (A) and entropy of activation ($\Delta S^{\#}$) have been calculated for each step, employing different integral methods of Doyle, Coats and Redfern, and Arrhenius. The reaction enthalpy is obtained from DSC data © 1998 Elsevier Science B.V.

Keywords: Cr(III) complexes; Octacyanomolybdate (IV); Octacyanotungstate (IV); Thermal decomposition; Thermal kinetics

---

1. Introduction

Different reports on thermal behaviour of chromium(III) molybdate exist in the literature. Plasova and Kefel [1] have found that $Cr_2(MoO_4)_3$ melts incongruently at 800–810°C and Getman and Marchenko [2] have reported that Chromium(III) molybdate in the solid state decomposes to Cr_2O_3 and MoO_3 before reaching its melting point. The decomposition of $Cr_2(MoO_4)_3$ starts at a temperature >850°C and is accompained by sublimation of MoO_3. Thermal degradation of group VI metal carbonyls have shown the influence of the metal and ligand on the decomposition course [3]. In complexes of the type $M(CO)_5L$ (where M=Cr, Mo and W, and L=pyridine, triphe-

---

*Corresponding author. Tel.: +91 683-1717; fax: +91 682-1232.

PII S0040-6031(98)00379-7

nylphosphine), TG and DSC studies have shown different expulsion behaviour of ligand with different metals [4].

Ultraviolet irradiation in the ligand field bands of the octacyanocomplexes of Mo(IV) and W(IV) in alkaline medium results in the substitution of cyanide ligand by water [5] which is followed by secondary thermal steps resulting in the loss of other cyanide groups with susequent formation of the stable products with other ligands such as 2,2′-bipyridyl, 1,10-phenanthroline, 1,2,3-benzotriazole, ethylenediamime and triethylenetetramine [6–9]. Ethylenediamine is reported to form a photoproduct with oxine [10] in which oxine- and cyano- moieties are removed in stages at higher temperatures resulting in the formation of an oxide of polymeric nature as residue. Thermal behaviour of various cyano compounds have shown that metal ions and the anion moieties affect the course of thermally induced reactions [11,12]. Since mixed ligand complexes of transition metals have been widely discussed, being biologically significant, the use of thermal methods of analysis to study the bonding and structure of coordination compounds are common [13]. We now report the formation of photo-substituted ethylenediamine complexes of $[M(CN)_8]^{4-}$ [where M=Mo(IV) or W(IV)] with chromium(III). The complexes are characterized by IR spectroscopy and thermal degradation has been studied by TG and DSC. The mechanism of the thermal dissociation has been proposed and thermodynamic parameters have been calculated employing different integral methods.

2. Materials and methods

Potassium octacyanomolybdate(IV) and octacyanotungstate(IV) were prepared by the method of Leipoldt et al. [14]. Ethylenediamine, chromium nitrate, $Cr(NO_3)_3{\cdot}6H_2O$ were of AR grade. All the solutions were prepared in doubly distilled water.

3. Synthesis of complexes

The complexes were synthesized by irradiating $K_4M(CN)_8$ [where M=Mo(IV) or W(IV)] and ethylenediamine solutions of 0.1 M strength in 1 : 2 ratio under UV radiation, until the colour of the solution changed to deep red. Irradiation was stopped at that stage and an aqueous solution of $Cr(NO_3)_3$ was added until the solution gave a black precipitate. The whole solution was subjected to centrifugation, the precipitates left were washed two to three times with water and then dried over fused $CaCl_2$. The complexes were analysed for C, H and N and the emperical formula for the complex **I** was found to be $Cr[Mo(CN)(C_2H_8N_2)(OH)_6]{\cdot}2H_2O$ **I** for Mo(IV): observed C=9.50; H=4.5; N=11.20% vs. calculated C=9.68; H=4.87; N=11.29% and$Cr[W(C_2H_8N_2)(O_2)(OH)_3].H_2O$ **II** for W(IV): observed C=6.50; H=3.3; N=7.25% vs. calculated C=6.05; H=3.3; N=7.05%.

4. Physical measurements

Determination of carbon, hydrogen and nitrogen was carried out by microanalysis. IR spectra of the complexes were recorded on a Perkin–Elmer 1710 Fourier-transform spectrophotometer in the 400-4000 cm^{-1} range using a KBr disc. The TG was conducted on a DuPont 2000 thermal analyser. DSC was also carried out on a DuPont TA 2000 system with a DSC attachment. The scanning was done at a rate of 10°C/min. An aluminium pan was used as reference under a dynamic nitrogen atmosphere. The DSC was calibrated by the fusion of indium (99.99% purity). The temperature repeatability of the instrument is ±0.1°C and of ΔH is ±0.02 mW.

5. Results and discussion

Photoexcitation of octacyano complexes of Mo(IV) and W(IV) with ethylenediamine results in the substitution of cyanide ions by ethylenediamine. Ethylenediamine provides a coordinating entity of amine group and forms complexes of different stoichiometries with Mo(IV) and W(IV). The IR absorption bands observed for complex **I** confirm the formation of metal–amine complex showing characteristic peaks at 3600, 1360, 880 cm^{-1} assigned as NH asymmetric deformation [15], NH symmetric deformation and the NH_3 rocking mode [16], respectively. The presence of cyanide group is shown by the characteristic C≡N stretching band at 2170–2040 cm^{-1}. Since the C≡N stretching band of the free ion in KCN is observed at 2080 cm^{-1} which is shifted to higher frequencies by coordination, and as coordination usually weakens the ligand bond next to the coordinate bond, thus shifting the ligand stretching vibrations to a lower frequency region [17], thus justifying the coordination of CN by appearance of the band at 2100 cm^{-1}. The band at 1050 cm^{-1} could be the result of the stretching vibration of either the C–N or C–C vibration. The band at ca. 1600 cm^{-1} may be assigned to the NH_2 vibrations. In addition to the C≡N stretching bond, the complex exhibits δ(M–C≡N) stretching at inner frequency region at 640–660 cm^{-1} which is in conformity with the reported δ(Cr–C≡N) [18]. The presence of water as lattice water trapped by weak forces is shown by the appearance of the symmetric (O–H) stretching mode at 3450 cm^{-1} (usually between 3550–3200 cm^{-1}) and of H–O–H bending mode at 1640 cm^{-1} (being between 1630–1600 cm^{-1}). The absorption band at 1500 cm^{-1} is due to –N=O or ring vibrations. The absoption peaks for the complex **II** are similar to that of the complex **I** with some variation in absorption peaks justifying the proposed composition. It shows the loss of absorption peaks due to C≡N stretching supporting the complete substitution of the cyanide ligand by ethylenediamine. The stretching vibration of C–C band is exactly the same at 1050 cm^{-1}. The N–H asymmetric deformation at 1600 cm^{-1} and NH_3 rocking mode at 840 cm^{-1} due to ethylenediamine molecule is also supportive of the metal–ammine complex. The σ_r (NH_3) in case of complex II is at lower frequency by 40 cm^{-1} than complex **I**, which may be due to the heavier mass of tungsten than molybdenum, shifting the M–N stretching vibration in lower frequency region. The presence of the water outside the coordination sphere is evident from the ν(O–H) mode at 3450 cm^{-1}, the same as in the complex **I**. The strong absorption at 1400 cm^{-1} is assigned as ν(–N=N–).

6. Thermogravimetry studies

6.1. $Cr[Mo(CN)(C_2H_8N_2)(OH)_6]\cdot 2H_2O$ I

The TG and DTG curves of complex **I** are shown in Fig. 1. The TG curve indicates the dissociation of the complex in two significant steps, the DTG shows a

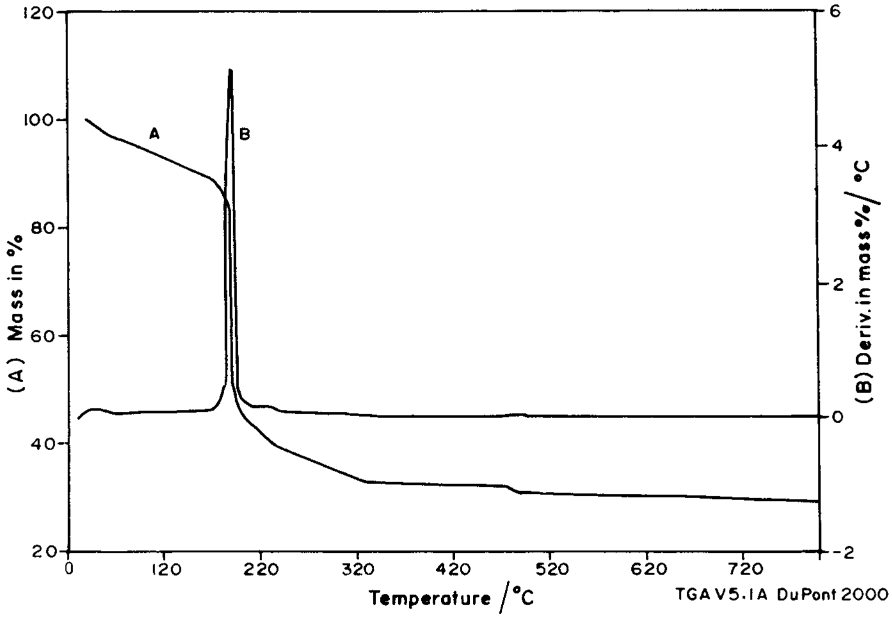

Fig. 1. The TG and DTG curves of complex **I**.

sharp peak corresponding to the second thermal decomposition step and a minor peak for the first transition.

The first transition initiates from 50 to170°C with DTG maximum of 110±0.1°C. The observed mass loss is 10.15, against the calculated loss of 9.68%, corresponding to the release of two moles of water. The temperature range of the transition and DTG maximum justifies the removal of water molcules from the outer coordination sphere. The second transition is a significant one starting from 180° to 280°C with DTG maximum of 230°C, undergoing an observed mass loss of 50.54 against the calculated loss of 50.7%, due to the release of the remaining coordinating moieties of 5 mol of hydroxyl, 1 mol of ethylenediamnine and 1 mol of cyanide. The observed mass of the residue is 39.15 against the calculated 39.7%, corresponding to mass of Cr and Mo metals. The sequential thermal decomposition process of the complex is shown in Scheme 1. The percentage with, and without, parentheses correspond to calculated and observed values, respectively.

$$Cr[Mo(CN)(C_2H_8N_2)(OH)_6].2H_2O \xrightarrow[10.15]{(9.68)}$$

$$Cr[Mo(CN)(C_2H_8N_2)(OH)_6] + 2H_2O \xrightarrow[50.70]{(50.54)}$$

$$Cr + Mo + 6OH + CN + C_2H_8N_2 \quad (39.7);\ 39.1\%$$

Scheme 1.

The DSC of **I** is shown in Fig. 2. Two transitions, one exothermic and one endothermic in DSC curve, correspond to the transitions observed in the TG curve. The exothermic transition observed due to the release of water molecules starts from 66.5°C up to 190.4°C with maximum at 151.0°C, giving ΔH value of 272.4 J/g. The endothermic transition observed due to the release of all other organic ligands and hydroxyl groups from the inner coordination sphere initiates from 200.5°C up to 297.7°C with maximum of 229.2°C involving a ΔH value of 174.8 J/g. The derivative of the second transition involves overlapping of the consecutive peaks, thus justifiing the evolution of more than one ligand. The mechanism involved is shown in Scheme 2.

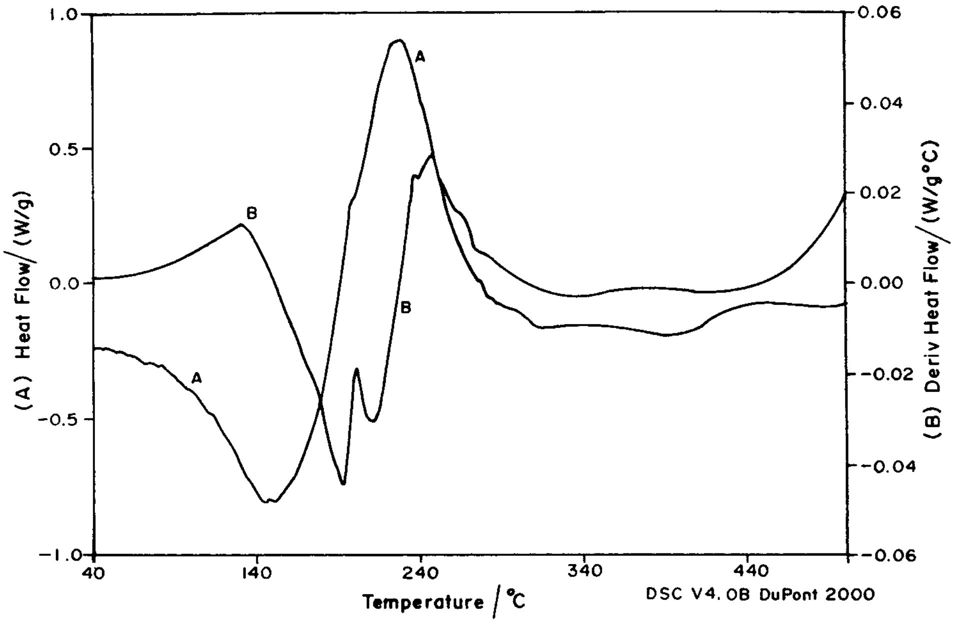

Fig. 2. The DSC curve of complex **I**.

$$Cr[Mo(CN)(C_2H_8N_2)(OH)_6].2H_2O \xrightarrow{\Delta H=272.4J/g}$$
$$Cr[Mo(CN)(C_2H_8N_2)(OH)_6] + 2H_2O \xrightarrow{\Delta H=174.8J/g}$$
$$Cr + Mo + 6OH + CN + C_2H_8N_2$$

Scheme 2.

6.2. $Cr[W(C_2H_8N_2)(O_2)(OH)_3]\cdot H_2O$ II

Here, the complex formation is somewhat different from that of complex **I**. The loss of the IR peaks of cyanide justifies the removal of all the cyanide ligands by different moieties. The TG along with DTG of the complex is shown in Fig. 3. The decomposition starts from 40°C and ends at 170°C with DTG maximum at 104.3°C showing the evolution of uncoordinated molecules of water and two hydroxyl groups in the form of the water molecules. The DTG maximum and temperature range support the expulsion of the moieties from the inner coordination sphere. The observed mass loss is 12.91 against calculated 13.10%. The second transition is in continuation with the first, starting from 180°C and ending at 310°C with DTG maximum of 217.2°C, involving a mass loss of 20.19 against calculated loss of 19.40%, corresponding to the release of one hydroxyl group and 1 mol of ethylenediamine molecule. The observed mass of the residue is 66.9 against calculated 67.4%, which is due to WO_2 and Cr metal. The decomposition temperature of WO_2 in nitrogen atmosphere being at 1550°C justifies it as residue. The mechanism showing different stages of decomposition is shown in Scheme 3. The percentages with, and without, parentheses correspond to the calculated and observed percentages, respectively.

The DSC of complex **II** is shown in Fig. 4. The transitions observed in the DSC curve correspond to the transitions observed in the TG curve. Three transitions, two exothermic and one endothermic, are observed. The first transition starts from 41.3°C and ends at 173.5°C with maximum of 133.0°C, giving a

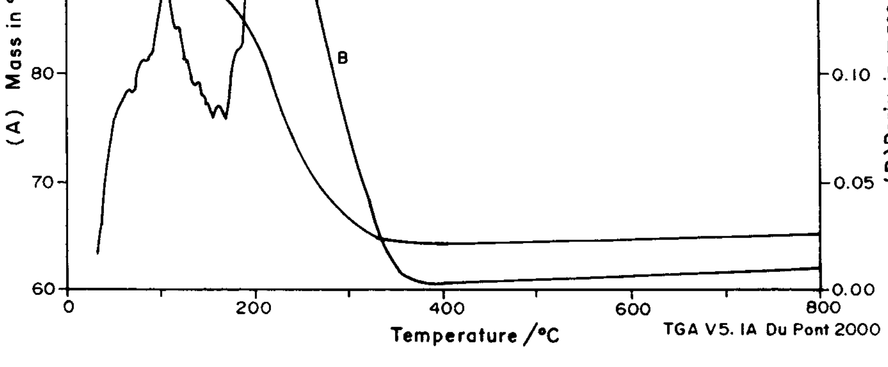

Fig. 3. The TG and DTG curves of complex **II**.

$$Cr[W(C_2H_8N_2)(O_2)(OH)_3]H_2O \xrightarrow[12.91]{(13.10)}$$
$$Cr[W(C_2H_8N_2)(O_2)(OH)] + 2OH + H_2O \xrightarrow[20.19]{(19.40)}$$
$$Cr + WO_2 + C_2H_8N_2 + OH\ (67.4);\ 66.9$$

Scheme 3.

$$Cr[W(C_2H_8N_2)(O_2)(OH)_3]H_2O \xrightarrow{\Delta H=101.3\ J/g}$$
$$Cr[W(C_2H_8N_2)(O_2)(OH)_3] + H_2O \xrightarrow{\Delta H=125.0\ J/g}$$
$$Cr[W(O_2)(OH)_3] + C_2H_8N_2 \xrightarrow{\Delta H=110.9\ J/g}$$
$$Cr[W(O_2)(OH)] + 2OH \xrightarrow{\Delta H=16.21 J/g} Cr + WO_2 + OH$$

Scheme 4.

ΔH value of 101.3 J/g. This exothermic transitions is due to the evolution of water molecules and hydroxyl groups. The second transition is an endothermic one involving a significant enthalpy value. This transition shows the evolution of ethylenediamine in two steps. The first endothermic peak starting from 184.8°C up to 263.9°C with maximum of 223.6°C involving ΔH value of 125.0 J/g. The second endothermic transition starts from 277.4°C up to 391.5°C with DTG maximum of 312.2°C involving ΔH value of 110.9 J/g. These endothermic peaks are followed by an exothermic transition starting from 420.9°C up to 472.9°C with maximum of 436.9°C which gives ΔH value of 16.21 J/g. The mechanism showing transitions with ΔH values are shown in Scheme 4.(Table 1)

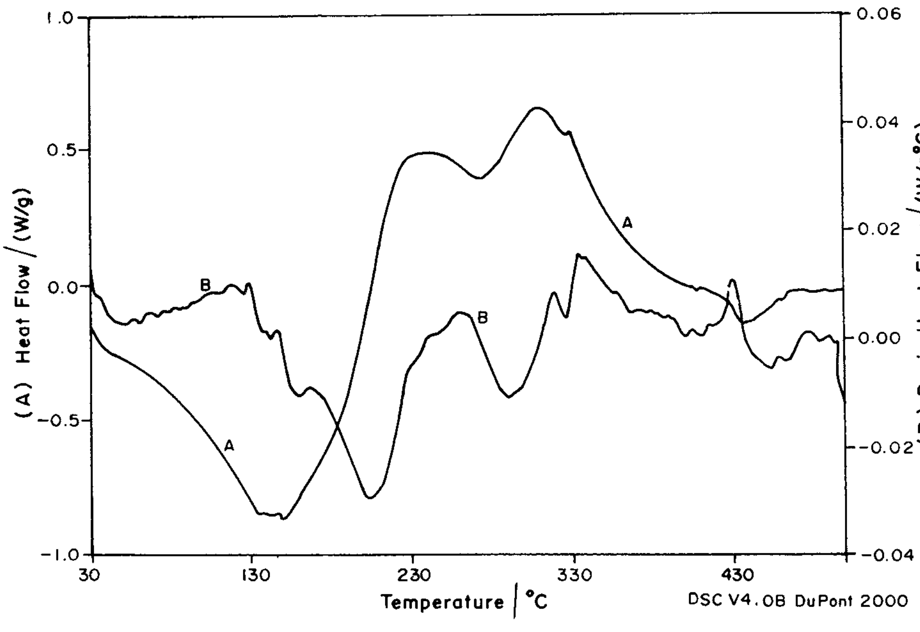

Fig. 4. The DSC curve of complex **II**.

Table 1
Thermoanalytical data for the decomposition of the complexes: $Cr[Mo(CN)(C_2H_8N_2)(OH)_6]\cdot 2H_2O$ **I** and $Cr[W(C_2H_8N_2)(O_2)(OH)_3]\cdot H_2O$ II

Temperature range/°C	Maximum temperature in DTG/°C	Observed mass loss/%	Calculated mass loss/%	Remarks: removal of
Complex **I**				
50–170	100.0(1)	10.15	9.68	2 mol of H_2O
180–280	200.0(1)	50.70	50.54	6 mol of OH+1 mol of $C_2H_8N_2$+1 mol of CN residue Cr+Mo; calculated (39.7); observed 39.15%
Complex **II**				
40–170	104.33(1)	12.91	13.10	1 mol of H_2O+2 mol of OH
180–310	217.17(1)	20.19	19.40	1 mol of OH+1 mol of $C_2H_8N_2$ residue Cr+WO_2: calculated 67.4; observed 66.9%

7. Kinetic parameters

Kinetic parameters calculated for different stages of decomposition of complexes **I** and **II** are given in Tables 2 and 3, respectively.

By using Doyle's [19] equation:

$$\log\frac{\rho_T}{w}=\frac{E_a}{4.6T}+\log\frac{A}{RH}$$

where $\rho_T=t/RH$, $-dw/dt$ the fraction decomposed at time 't', R the gas constant, H the heating rate, w the weight of the sample at time 't', E_a the activation energy, A the frequency factor, and T the temperature in Kelvin. Plot of log ρ_T/w vs. $1/T$ gives a straight line for a first-order reaction. The best fit equation obtained from programme Grapher (ver 1.20) from which activation energy (E_a) is obtained as he slope of the

Table 2
Activation energy, frequency factor and entropy of activation for $Cr[Mo(CN)(C_2H_8N_2)(OH)_6]\cdot 2H_2O$ **I**

Stage	Parameters	DTG maximum temperature/K	Doyle	Coats and Redfern	Arrhenius
I	E_a/(kJ mol^{-1})		20.9	10.9	24.0
	A/(s^{-1})	373.0	1.6	4.9	0.6
	$\Delta S^{\#}$/(J K^{-1} mol^{-1})		−243.0	−233.6	−250.9
II	E_a/(kJ mol^{-1})		19.4	1.0	10.0
	A/(s^{-1})	573.0	1.7	5.3	0.1
	$\Delta S^{\#}$/(J K^{-1} mol^{-1})		−245.9	−232.9	−266.3

Table 3
Activation energy, frequency factor and entropy of activation for the $Cr[W(C_2H_8N_2)(O_2)(OH)_3]\cdot H_2O$ **II**

Stage	Parameters	DTG maximum temperature/K	Doyle	Coats and Redfern	Arrhenius
I	E_a/(kJ mol^{-1})		23.5	18.1	26.3
	A/(s^{-1})	377.3	2.0	3.9	1.5
	$\Delta S^{\#}$/(J K^{-1} mol^{-1})		−241.1	−235.8	−243.7
II	E_a/(kJ mol^{-1})		21.2	15.2	22.3
	A/(s^{-1})	490.2	1.6	4.4	0.8
	$\Delta S^{\#}$/(J K^{-1} mol^{-1})		−245.4	−236.8	−250.9

equation using the relation $E_a = -4.6\times\text{slope}$ and pre-exponential factor (A) from the intercept of the plot. The entropy of the activation ($\Delta S^{\#}$) is obtained from the following equation:

$$A = \frac{kT_s}{h}\exp\left(\frac{\Delta S^{\#}}{R}\right) \tag{A}$$

where k is the Boltzmann constant, h the Planck

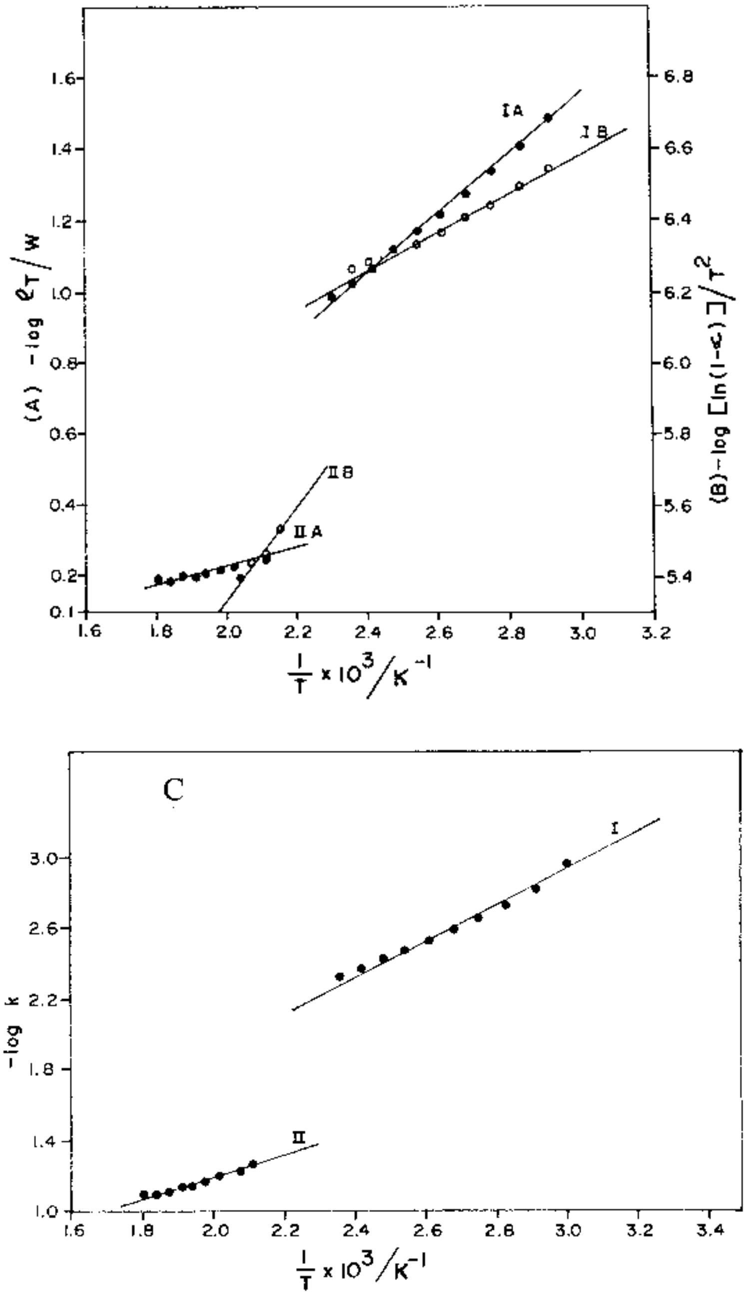

Fig. 5. Plot of $-\log \rho_T/w$ vs. $1/T\times10^3$ K^{-1} of complex **I**.

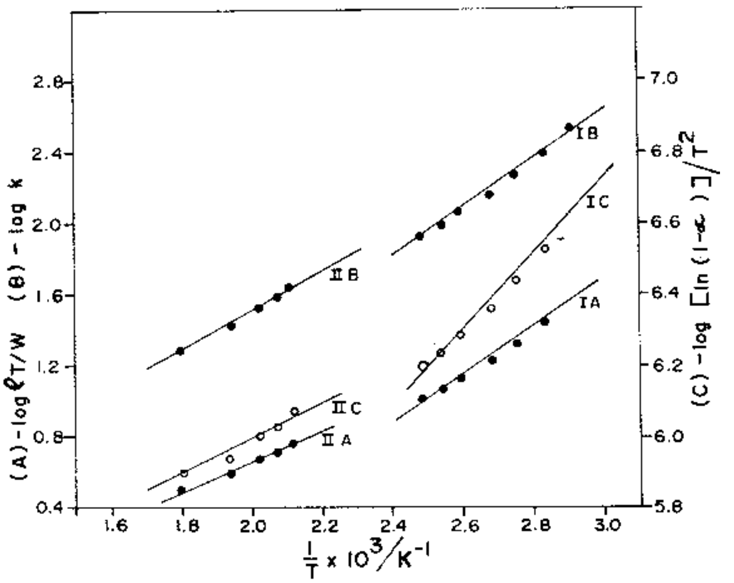

Fig. 6. Plot of $-\log k$ vs. $1/T\times10^3$ K^{-1} of complex **I**.

constant and T_s the DTG peak temperature. The Coats and Redfern [20] equation for n=1 is given as follows:

$$\log\left[\frac{\log(1\alpha)}{T^2}\right] = \log\frac{AR}{HE_a}\left[1-\frac{2RT}{E_a}\right] - \frac{E_a}{2.3RT}$$

where α is the fraction decomposed at time 't', E_a the activation energy, H the heating rate, R the gas constant and A the pre-exponential factor was also used. A plot of $\log[-\ln(1-\alpha)]/T^2$ vs. $1/T$ for n=1 was linear for each stage of decomposition of complex **I** (Fig. 5(b)) and complex **II** (Fig. 6(b)) obtained by programme Grapher. The activation energy (E_a) and frequency factor (A) was obtained from the slope and intercept of the best fit equation of the plot, respectively. Arrhenius [21] equation was also employed for the determination of kinetic parameters using equation$-\mathrm{d}x/\mathrm{d}t = kx^n$, where x is the amount of the sample undergoing reaction, n the order of the reaction and k the specific rate constant. The best fit equation of the plot of log k vs. $1/T$ gave slope and intercept from which the values of E_a and A were obtained.

From Tables 2 and 3, the values of E_a and $\Delta S^{\#}$ of a particular stage using different methods are comparable, although the values obtained by Coats and Redfern's lie on the lower side. The negative values of $\Delta S^{\#}$ indicate that the activated complexes have a ordered structure than the reactants and the reactions are slower than normal [22].

From Table 1, it is evident that activation energy is maximum for the first step and minimum for the second step. The corresponding value of entropy of activation is also maximum for step **I** and minimum for step **II**. Since Lozano [23] found that greater enthalpy and lower activation energy are responsible for greater binding between pyridine and molybdenum atom in the complexes, here, the low activation energy is observed in the second step, and involves release of ethylenediamine and hydroxyl group, attributing towards greater stability, hence being removed at the latter stages in the decomposition process. The same trend is observed for complex **II**, where the thermodynamic parameters show greater coordination of ethylenediamine and hydroxyl group with the tungsten metal, being removed in the last step of the thermal decomposition.

Acknowledgements

One of the authors Kowsar Majid is grateful to CSIR, New Delhi for the award of Senior Research Fellowship.

References

[1] L.M. Plasova, L.M. Kefeli, Izv. Akad. Nauk. SSSR, Neorg. Mater. 3 (1967) 906.

[2] E.J. Getman, V.J. Marchenko, Zh. Neorg. Khim. 28 (1983) 713.

[3] T.S.A. Hor, H.S.O. Chan, C.S.M. Chiam, K. Hivalemi, Thermochim. Acta 128 (1988) 175.

[4] H.S.O. Chan, T.S.A. Hor, J.R. Lusty, K.H. Lim, C.S.M. Chiam, J. Therm. Anal. 34 (1988) 121.

[5] V. Balzani, V. Carrassiti, Photochemistry of Coordination Compounds, Academic Press, London, New York, 1970.

[6] S.I. Ali, H. Kaur, Transition Met. Chem. 17 (1992) 304.

[7] S.I. Ali, H. Kaur, Bull. Chem. Soc. Jpn. 63 (1990) 3615.

[8] S.I. Ali, A. Kumar, J. Photochem. Photobiol. A: Chem. 72 (1993) 29.

[9] S.I. Ali, H. Kaur, Transition Met. Chem. 16 (1991) 450.

[10] S.I. Ali, A.M.A. Ansari, J. Therm. Anal. 46 (1996) 1763.

[11] D. De Marco, A. Marchese, P. Migliardo, A. Bellomo, J. Therm. Anal. 32 (1987) 919.

[12] S.B. Seifer, Russ. J. Inorg. Chem. 5 (1960) 33; 8 (1963) 762; 8 (1963) 607.

[13] W.W. Wendlandt, J.P. Smith, The Thermal Properties of Transition Metal Ammine Complexes, Elsevier Amsterdam, 1967.

[14] L.G. Leipoldt, L.D.C. Bok, P.I. Colliers, Z. Anorg. Allg. Chem. 409 (1974) 343; 407 (1974) 250.

[15] S. Mizushima, I. Nakagava, J.V. Quagliana, J. Chem. Phys. 23 (1955) 136.

[16] G.M. Barrow, R.H. Krenger, F. Basolo, J. Inorg. Nucl. Chem. 2 (1956) 2340.

[17] K. Nakamoto, Infrared Spectra of Inorganic and Coordination Compounds, NY, 1963, pp 167.

[18] V. Caglioti, G. Sartori, C. Furtani, J. Inorg. Nucl. Chem. 13 (1960) 22.

[19] C.D. Doyle, J. Appl. Polym. Sci. 15 (1958) 394.

[20] A.W. Coats, J.P. Redfern, Nature (London) 201 (1964) 68.

[21] J.R. Hullet, Quart. Rev. 18 (1964) 227.

[22] A. Frost, R.G. Pearson, Kinetics and Mechanism, Wiley, NY, 1961.

[23] R. Lozano, A. Moragues, J. Roman, Thermochim. Acta 108 (1986) 1.